glycine receptors (Fig. 3D). This design accounts for the pre- and postsynaptic effects of 5HT (Fig. 3E) observed in our study.

Various mechanisms—for example, a decrease in K^+ conductances (*1*) or an increase in Ca^{2+} conductances (*17*) and in intracellular Ca^{2+} contents (*18*)—could account for these observations. Several lines of evidence, from 12 additional experiments, point toward an involvement of K^+ channels. These results showed that 5HT has opposite effects on (presumably different) K^+ channels in the M cell and in the presynaptic terminals. Postsynaptically, 5HT opened K^+ conductances that showed inward rectification (*19*) and were blocked by Cs ions (2 to 5 m*M*; $n = 7$). At the presynaptic terminal, 5HT, as well as K^+ channel blockers such as Cs (2 to 5 m*M*; $n = 7$) and tetraethylammonium (1 m*M*; $n = 5$), increased synaptic noise.

Facilitation of excitatory transmitter release by 5HT (*5, 20*) has been implicated in sensitization in *Aplysia* (*1*), whereas in other systems this amine may have a net inhibitory effect, such as with the restraint inhibition of the crayfish escape reflex (*21*). Our results define a structural locus for this type of modulation that is restricted to the presynaptic terminals and distant from the soma of the interneuron (*7*). They thus extend the notion of facilitated release to inhibitory networks and suggest that a reinforcement of glycine transmission might underlie habituation (*22*) of M cell–mediated escape reactions.

REFERENCES AND NOTES

1. E. R. Kandel and J. H. Schwartz, *Science* **218**, 433 (1982).
2. D. A. Baxter, G. D. Bittner, T. H. Brown, *Proc. Natl. Acad. Sci. U.S.A.* **82**, 5978 (1985); K. Kuba and E. Kumamoto, *J. Physiol. (London)* **374**, 515 (1986).
3. W. J. Davis, R. Gillette, M. P. Kovac, R. P. Croll, E. M. Matera, *J. Neurophysiol.* **49**, 1557 (1983).
4. W. Wouters and J. van den Bercken, *Nature* **277**, 53 (1979).
5. W. Finger and C. Martin, *Neurosci. Lett.* **51**, 127 (1984).
6. Y. Nakajima, *J. Comp. Neurol.* **156**, 375 (1974).
7. A. Triller and H. Korn, *J. Neurophysiol.* **48**, 708 (1982).
8. T. Furukawa and E. J. Furshpan, *ibid.* **26**, 140 (1963).
9. H. Korn and D. S. Faber, *Science* **194**, 1166 (1976).
10. D. S. Faber and H. Korn, in *Neurobiology of the Mauthner Cell*, D. S. Faber and H. Korn, Eds. (Raven, New York, 1978), pp. 47–131.
11. H. Korn, A. Mallet, A. Triller, D. S. Faber, *J. Neurophysiol.* **48**, 679 (1982).
12. H. Korn, Y. Burnod, D. S. Faber, *Proc. Natl. Acad. Sci. U.S.A.* **84**, 5981 (1987).
13. J. A. Benson and I. B. Levitan, *ibid.* **80**, 3522 (1983); J. L. Yakel, L. O. Trussel, M. B. Jackson, *J. Neurosci.* **8**, 1273 (1988).
14. Excitatory currents are also inward-going in voltage-clamped Cl^--loaded cells. However, their contribution to the background noise was insignificant because it was almost completely absent (i) when recorded with potassium acetate electrodes at resting potential, which is close to the Cl^- equilibrium potential in the M cell (*8*), and (ii) in the presence of strychnine applied iontophoretically (18 m*M*) or by intraperitoneal injections (2 to 4 μg per gram of body weight).
15. P. A. M. Van Dongen *et al.*, *J. Comp. Neurol.* **234**, 501 (1985).
16. Y. Nakajima and K. Kohno, in *Neurobiology of the Mauthner Cell*, D. S. Faber and H. Korn, Eds. (Raven, New York, 1978), pp. 133–166.
17. D. Paupardin-Tritsch, C. Hammond, H. M. Gerschenfeld, *J. Neurosci.* **6**, 2715 (1986).
18. D. B. Pritchett *et al.*, *EMBO J.* **7**, 4135 (1988).
19. D. S. Faber and H. Korn, *Neuroscience* **19**, 1037 (1986).
20. S. Glusman and E. A. Kravitz, *J. Physiol. (London)* **325**, 223 (1982).
21. D. L. Glanzman, and F. B. Krasne, *J. Neurosci.* **6**, 1560 (1986).
22. R. C. Eaton, R. D. Farley, C. B. Kimmel, E. Schabtach, *J. Neurobiol.* **8**, 151 (1977).
23. O. Kah and P. Chambolle, *Cell Tissue Res.* **234**, 319 (1983).
24. A. Triller, F. Cluzeaud, F. Pfeiffer, H. Betz, H. Korn, *J. Cell Biol.* **101**, 683 (1985).
25. S. M. Hsu, L. Raine, H. Fanger, *J. Histochem. Cytochem.* **29**, 577 (1981).
26. B. Schmitt, P. Kanaus, C. M. Becker, H. Betz, *Biochemistry* **26**, 805 (1987).

27. Support was provided by INSERM and by Fondation pour la Recherche Médicale.

12 December 1988; accepted 1 May 1989

Neural Connections Between the Lateral Geniculate Nucleus and Visual Cortex in Vitro

NOBUHIKO YAMAMOTO, TOHRU KUROTANI, KEISUKE TOYAMA

Neural connections were established in cocultures of rat visual cortex (VC) and lateral geniculate nucleus (LGN), which were isolated in early infancy. Morphological and electrophysiological studies showed that the cortical laminar organization of afferent and efferent connections in the coculture preparations was similar to that in the adult VC. The results indicate the existence of intrinsic mechanisms in VC and LGN that guide the formation of synaptic connections with the appropriate targets.

THE QUESTION OF HOW SPECIFIC neural connections in neocortical structures are established during development has been one of the central problems in neurobiology. The visual cortex (VC), characterized by well-developed laminar organization of neural connections (*1, 2*), is the optimal material for studies that address this question. Because the laminar organization is immature at birth and develops in the early postnatal life of the animal, there should be mechanisms in infant VC that guide axonal extension and synapse formation with appropriate targets to produce stereotyped laminar structures (*3–5*). We investigated the mechanisms underlying the specific neural connections between VC and lateral geniculate nucleus (LGN) by using a coculture technique (*6*). Our results demonstrate that neural connections with laminar specificity can be established in LGN-VC cocultures, suggesting the existence of intrinsic mechanisms that control axonal growth and synaptogenesis.

Whole blocks of LGN (0.8 mm by 0.6 mm by 0.3 mm) were dissected from 16- to 17-day-old rat fetuses, which were removed from the mother (Sprague-Dawley) under pentobarbital anesthesia (*5, 7*). VC slices (0.3 to 0.5 mm thick) were dissected from 1- to 3-day-old rats. A pair of the LGN and VC were plated on a culture dish with a collagen-coated membrane (Coster, Transwell-Col) in serum-free, hormone-supplemented medium (*8*). The LGN explant was placed in contact with or at a distance of <0.5 mm to the ventral surface of the VC explant. The cultures were maintained at 37°C in humidified 95% air and 5% CO_2.

Massive neurite connections developed between the LGN and VC explants in 37 of 59 cocultures (Fig. 1A). Morphological and electrophysiological studies were usually conducted after 2 to 3 weeks in culture. Nissl-stained sections of the VC explant demonstrated laminar and columnar organization composed of pyramidal or granular cells (Fig. 1B), which resembled that of normal rat VC (Fig. 1C). There was not much difference in the cell size (10 to 20 μm) between the VC explant and normal VC. However, the entire cortical thickness of the VC explant was commonly slightly smaller than that of the normal VC (Fig. 1, B and C). This seems to be attributable to thinner supragranular layers, suggesting retardation in development of these layers.

Neuronal connections between the LGN and VC explants were studied in 13 cocultures by antero- and retrograde labeling with horseradish peroxidase (HRP) or a fluorescent dye (DiI, Molecular Probes) (*4, 9, 10*). HRP-anterograde labeling of the LGN axons, with very few retrogradely labeled VC cells is shown in Fig. 1D. Most of the labeled axons extended along the columnar structure in the VC and branched in and around the granular layer. Anterograde labeling with DiI showed the axonal arboriza-

Department of Physiology, Kyoto Prefectural School of Medicine, Kawaramachi-Hirokoji, Kyoto 602, Japan.

tion and bouton-like swellings (Fig. 1E), which were analogous to the morphology of the normal geniculate axons (*11*).

In other instances there was preferential HRP-retrograde labeling of the VC cells (Fig. 1F). The labeled cells were most frequently encountered in the lower half of the infragranular layers, less frequently in the upper half, and very rarely in the supragranular and granular layers. Altogether, the major morphological features of the VC explant, such as cell size and laminar organization of neural connections, were comparable to those in the adult VC (*1*). Likewise, neuronal size and morphology in the LGN explant resembled those in the normal LGN (*12*).

The neural connectivity between the LGN and VC explants was investigated electrophysiologically with a method similar to that used in the VC slice preparations (*5, 13, 14*). Field potentials (FPs) evoked by stimulating the LGN explant were prominent in the granular layer of the VC explant in all six cases (traces FP in Fig. 2A). The current source-density (CSD) analysis of the FPs revealed current sinks (hatched area in traces CSD), representing excitatory synaptic transmission (*15*). The current sinks contained the early and late components discriminated according to the critical latency (dashed line in traces CSD) for mono- and polysynaptic transmission, which was inferred from the latency-distance relation in intracellular responses (*16*). The early currents were distributed around the granular layer, whereas the late currents were rather dominant in the supragranular layers. This distribution resembled that of the normal VC (Fig. 2B) and LGN-VC transplant preparations (*5*), except that late currents were considerably smaller in the cocultures than those in the normal VC (Fig. 2, A and B). Furthermore, possible contribution of the VC efferent to the LGN-evoked responses was investigated in the control experiments (n = 4), in which LGN-VC connections were transected and CSD analysis was performed 2 days after the transection by stimulating the proximal cut end. It was found that the early currents in the granular layer almost disappeared, although there were current sinks in the supra- and infragranular layers probably mediated by cortical efferents (Fig. 2C). Therefore, at least the early currents occurring in the granular layer of the cocultured VC seem to reflect the effects mediated by the LGN axons rather than those mediated by the VC efferents.

The mode of the neural connections was studied further by intracellular recording from 38 cells in nine VC explants. LGN stimulation produced three types of postsynaptic potentials: (i) a sequence of an excitatory postsynaptic potential (EPSP) and an inhibitory postsynaptic potential (IPSP) in 19 of 34 cells (Fig. 2D), (ii) an EPSP alone in 10 of 34 cells (not shown), and (iii) an IPSP alone in 5 of 34 cells (not shown). In many cells these EPSPs were large enough to initiate orthodromic spikes (Fig. 2E).

Latencies of the postsynaptic responses varied among individual cells (EPSP latencies, 3 to 9 ms; IPSP latencies, 4 to 14 ms). In layers II, III, and IV (*17*), a clear linear relation was found in each layer between EPSP latencies and distances between the stimulation and recording sites. The slopes (± SE) of the latency-distance relation representing the reciprocal of the conduction velocity of the LGN axons were roughly the same (2.8 ± 1.5, 3.0 ± 0.4, and 3.0 ± 0.5 s per meter in layers II, III, and IV, respectively), whereas the intersections representing the central delays (delay for synaptic transmission in VC) were different according to the layers (1.8 ± 0.8 ms, 1.1 ± 0.4 ms, and 0.9 ± 0.5 ms in layers II, III, and IV, respectively). The central delays suggest that

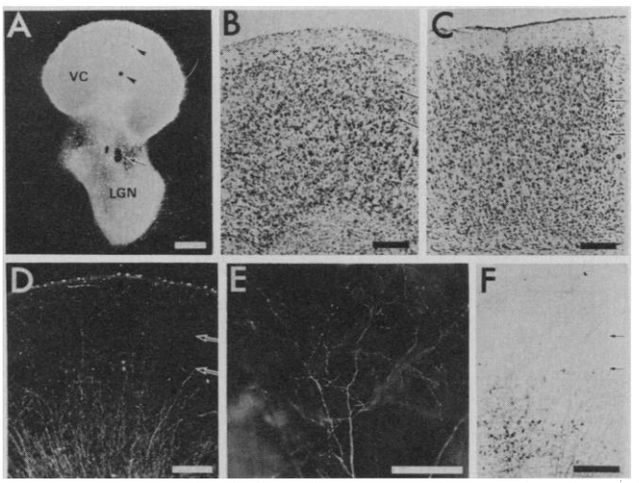

Fig. 1. Histological pictures of LGN-VC coculture. (**A**) Dark-field picture of LGN and VC explants. Arrowheads indicate the dye marks placed at two recording sites. The arrow indicates the stimulation site. (**B**) A Nissl-stained section (25 μm) of the VC explant (2 weeks in vitro) in comparison with 3-week-old normal VC (**C**). (**D**) Dark-field picture of LGN axons anterogradely labeled with HRP. (**E**) Arborization of a DiI-labeled LGN axon in the granular layer. (**F**) Cells retrogradely labeled with HRP in the VC. Upper and lower arrows in (B to D and F) indicate the supragranular-granular and granular-infragranular borders; (A) 7 days and (B and D to F) 14 to 18 days in vitro; bars: 500 μm in (A), 200 μm in (B to D and F), and 100 μm in (E).

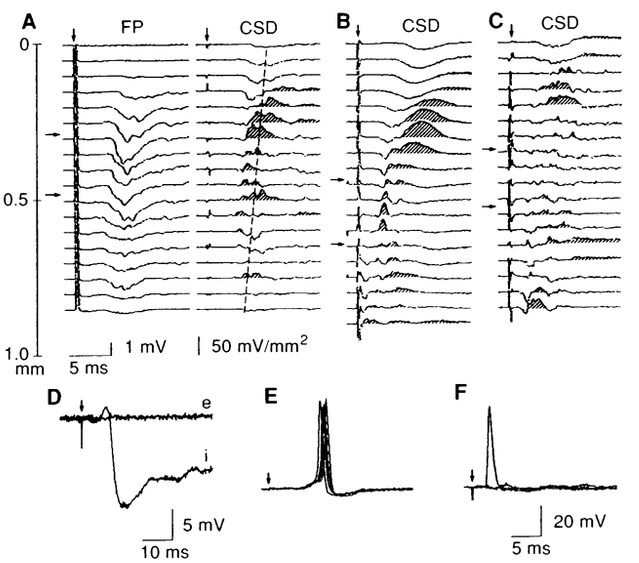

Fig. 2. Extra- and intracellular responses evoked in the VC explant by LGN stimulation. (**A**) FPs (traces labeled FP) and CSDs (traces labeled CSD). CSDs were determined as second-order spatial differentials of the FPs. The culture period was 14 days. Each FP and CSD trace represents an average of ten records. Sampling interval, 0.05 mm. Differentiation grid for CSD analysis, 0.15 mm. Upward deflections in traces FP and CSD represent positivity and current sinks (hatched area), respectively. The dashed line through CSD traces indicates the critical latency. The cortical depth of recording and the supragranular-granular (upper horizontal arrow) and granular-infragranular borders (lower arrow) are indicated to the left. In (**B**) the CSDs were similar to (A), but evoked in the normal rat (21-day-old) VC slice by white matter stimulation. (**C**) Similar CSDs were obtained in the control experiment, where the LGN-VC connections of the coculture (16 days in vitro) were severed and CSD analysis was conducted 2 days after the severance by stimulation of the proximal cut end. The calibration for CSDs was the same in (A) to (C). (D to F) Intracellular responses in VC cells after 16 to 18 days in vitro. (**D**) Postsynaptic potential (trace i) and extracellular field potential (trace e). The traces represent an average of four records. (**E**) Orthodromic spikes. (**F**) Antidromic spikes. Each (E) and (F) trace represents four superposed records. Time and voltage calibrations of 10 ms and 5 mV apply to (D), and those of 5 ms and 20 mV to (E) and (F). Stimulus intensities and durations, 0.5 to 1.5 mA and 0.1 ms. The arrows indicate the moment of stimulation.

EPSPs in layers III and IV and those in layer II represent mono- and polysynaptic transmissions, respectively. A similar relation was found in IPSPs of layer II to IV cells, but with a greater slope (4.2 ± 0.7 s per meter) and central delay (2.7 ± 1.4 ms), suggesting the polysynaptic nature of IPSPs. Besides the orthodromic responses, LGN stimulation produced antidromic spikes in about one-third of the infragranular layer cells (Fig. 2F).

The results of the intracellular responses were in agreement with those reported for adult VC (*2*) and LGN-VC transplant preparations (*5*), except that conduction velocity of the LGN axons was much slower (*2, 18*).

In summary, morphological and electrophysiological studies indicate that neural connections are mutually established between the cocultured LGN and VC, preserving laminar organization of afferent and efferent, and excitatory and inhibitory connectivity. Our findings indicate the existence of intrinsic mechanisms yielding appropriate axonal extension and synapse formation in LGN and VC.

REFERENCES AND NOTES

1. A. Peters and M. L. Feldman, *J. Neurocytol.* **5**, 63 (1976); J. S. Lund, G. H. Henry, C. L. Macquenn, A. R. Harvey, *J. Comp. Neurol.* **184**, 599 (1979); C. D. Gilbert, *Annu. Rev. Neurosci.* **6**, 217 (1983).
2. K. Toyama, K. Matsunami, T. Ohno, S. Tokashiki, *Exp. Brain Res.* **21**, 45 (1974).
3. R. W. Sperry, *Proc. Natl. Acad. Sci. U.S.A.* **50**, 703 (1963); P. Weiss, *J. Exp. Zool.* **68**, 393 (1934); R. D. Lund and M. J. Mustari, *J. Comp. Neurol.* **173**, 289 (1977); C. J. Shatz and M. P. Stryker, *Science* **242**, 87 (1988).
4. Y. Komatsu *et al.*, *Dev. Brain Res.* **22**, 305 (1985).
5. Hamasaki *et al.*, *Brain Res.* **422**, 172 (1987).
6. S. M. Crain, in *Cell, Tissue, and Organ Cultures in Neurobiology*, S. Fedoroff and L. Hertz, Eds. (Academic Press, New York, 1977), pp. 147–190; B. H. Gähwiler, *J. Neurosci. Methods* **4**, 329 (1981).
7. The dissected block was confirmed to contain the entire LGN as well as a part of other thalamic nuclei (roughly one-third of the dissected block) in histological sections of the fetal brain from which the LGN block was dissected.
8. G. Brunner *et al.*, *Dev. Brain Res.* **2**, 563 (1982).
9. A small piece of HRP crystal was applied to a fine incision made in the connection between the LGN and VC explants. After 2 to 4 hours of incubation, the culture was fixed and reacted with diaminobenzidine.
10. A piece of DiI was placed on the surface of the LGN of coculture preparations fixed with formalin, and the cultures were kept for 3 to 7 days at room temperature to allow diffusion of the dye. This always yielded preferential anterograde labeling of LGN axons with very scarce labeling of VC cells [P. Godement, J. Vanselow, S. Thanos, F. Bonhoeffer, *Development* **101**, 697 (1987)].
11. D. Ferster and S. LeVay, *J. Comp. Neurol.* **182**, 923 (1978).
12. J. G. Parnavelas, E. J. Mounty, R. Bradford, A. R. Lieberman, *ibid.* **171**, 481 (1977).
13. Y. Komatsu *et al.*, *J. Neurophysiol.* **59**, 124 (1988).
14. Spontaneous discharges were not detected in the LGN and VC explants by extracellular recording.
15. C. Nicholson and J. A. Freeman, *J. Neurophysiol.* **38**, 356 (1975).
16. The critical latency was determined as a sum of conduction time of afferent impulses and the median value (1.5 ms) of the central delays for mono- and polysynaptic EPSPs. The conduction time was calculated according to the conduction velocity of LGN impulses (0.33 m/s) and the distances between the stimulation and recording sites.
17. The upper and lower halves of the supragranular layers and the granular layer were referred to as layer II, III, and IV, respectively.
18. Y. Fukuda, I. Sumitomo, C.-F. Hsiao, *J. Neurophysiol.* **50**, 46 (1983).

19. We thank H. Fujisawa and S. Takagi for their useful advice and for permitting us to use their laboratory equipment, and Y. Komatsu and F. Murakami for their helpful advice. Supported by grants-in-aid for Scientific Research Projects 63770091 and 63112006 from the Japanese Ministry of Education, Science, and Culture.

28 November 1988; accepted 8 May 1989

Technical Comments

Ultraviolet Levels Under Sea Ice During the Antarctic Spring

J. E. Frederick and H. E. Snell report (*1*) that the extended period of summertime ultraviolet (UV) radiation levels in the Antarctic during the period of ozone depletion may be harmful to indigenous life forms. It was pointed out that since the local life forms may have developed only the minimum defenses necessary to tolerate the UV levels in which they evolved, it is reasonable to consider the fractional increase in the local yearly dose as a measure of potential damage. It is therefore alarming that the presented estimates of the UV radiance during October and November at McMurdo Sound were as large as those in mid-summer.

The purpose of this comment is to point out that the spring UV enhancement will be exaggerated under the vast sea ice cover surrounding Antarctica, an environment rich in life. This conclusion follows from experiments (*2–5*) which clearly show that the ice is less turbid in early spring than later in the season. The increased turbidity in late spring results from the growth of weakly scattering brine inclusions as the ice warms and from the strongly scattering air channels left near the surface as brine drains into the bulk of the ice (*4*). To date, transmission measurements have been made only in the visible part of the spectrum, but modeling of the diffusive transport of light through sea ice (*3, 5*) permits extrapolation into the UV, relying only on the UV absorption coefficient of pure ice. This coefficient is not accurately known, but estimates based on measurements on water (*6*) suggest a value of about 0.2 m^{-1} at 300 nm. For an absorption coefficient in this range, we have found that the radiance transmitted through the ice falls from ~0.75% in early November to ~0.25% 3 weeks later. As a guide to evaluating the transmission beyond this period, we note that the measured (*8*) under-ice solar radiance in early October implies a 5% transmission at a wavelength (620 nm) for which the absorption coefficient is 0.2 m^{-1}. To estimate transmission of the ice after 20 November, we consider two limits: (i) there

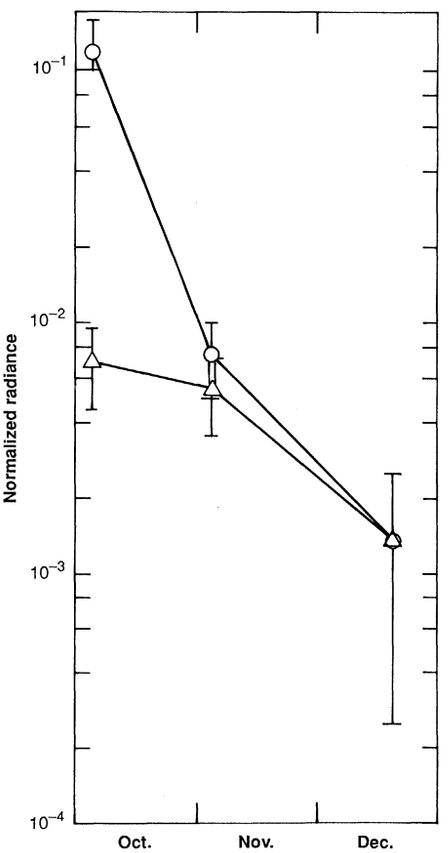

Fig. 1. A plot of the temporal development of the UV radiance at 305 nm under sea ice normalized to the surface radiance on 21 December (*1*). The lower curve (△) is for an unperturbed ozone layer assuming 315 Dobson units (DU). The upper curve (○) demonstrates the 20-fold increase in UV transmission during the presence of the ozone hole, assuming a changing ozone atmosphere, that is, 110 DU (5 October), 250 DU (5 November), and 315 DU (21 December) (*1*). The error bars on the point for 21 December cover the two turbidity limits discussed in the text. The error bars on the other points result from variations we have encountered in sea ice transmission.